Study of the nonequilibrium state of superconductors by large quasiparticle injection from an external current source

I. Iguchi

Department of Mathematical Engineering and Instrumentation Physics, University of Tokyo, Tokyo, Japan

(Received 4 January 1977; revised manuscript received 22 April 1977)

We have studied the nonequilibrium state of superconductors by injecting large numbers of quasiparticles from an external current source into a superconducting film of a tunnel junction with low tunnel resistance (typically 0.1–1 Ω for junction area $\simeq 10^{-4}$ cm^2). It was observed that there was a critical tunnel current density at which a voltage appeared locally in the part of a superconducting film confined to the junction area. Its values ranged from 10^2 to 10^3 A/cm^2 for bath temperatures well below T_c. Followed by this voltage onset, a transition region corresponding to the nonequilibrium intermediate resistive state was also observed. For further increase of the tunnel current, the local film resistance developed beyond the value of its normal resistance, suggesting that the nonequilibrium state extends far beyond the voltage onset point. A theory based on the modified Rothwarf-Taylor equations and Parker's T^* model is presented to compare with the experimental results. The calculated critical current density yielded almost the same order of magnitude as those found experimentally. The detailed behavior, however, deviates from the theoretical predictions although the film makes a second-order transition in the broad range of temperatures. It is also shown using four-terminal analysis that our observations and those by Wong, Yeh, and Langenberg are essentially the same.

I. INTRODUCTION

It has been demonstrated in recent years that quasiparticle injection into a superconducting film by some means drives it locally to the nonequilibrium state. Its appearance in both the small and large injection regimes provides new possibilities for application to superconductors as well as for their basic study. In the nonequilibrium state, several dynamic processes are involved: the inelastic scattering of quasiparticles with phonons, the recombination of quasiparticles with the emission of phonons to form ground-state pairs, the phonon escape from the surface of superconductors, etc. Photons, phonons, and quasiparticle tunnel current have been used as external sources of quasiparticle injection so far.[1]

In the case of photoinjection, Testardi[2] first observed the appearance of a dc resistance in superconducting lead films using pulsed laser light. He concluded that this could not be ascribed to simple heating. Then similar measurements were intensively performed by many authors[3-10] in both the small- and large-injection regimes. For the latter case, they observed the continuous decrease of the gap parameter with an increase of light intensity and a second-order transition to the normal state.

In the case of dynamic pair breaking by phonons, much[11-13] has been done in connection with phonon spectroscopy.

In the small-injection-current regime there are experiments[14-22] using a two-tunnel-junction configuration to measure the effective recombination time of quasiparticles. In the large-injection-current regime, Yeh and Langenberg[23] observed an appreciable decrease of the superconducting energy gap in the tunneling characteristic of high-current-density Sn tunnel junctions. They concluded that the effect could not be accounted for by simple heating. Wong, Yeh, and Langenberg[24] have recently made quasiparticle-injection-induced superconducting weak links by giving two independent current flows in the superconducting film of a tunnel junction, one just flowing through the film, the other flowing across the junction. With the tunnel current biased at a certain level, they could successfully observe Josephson weak-link behavior. They also reported that there was a critical tunnel current above which the current-voltage characteristics did not exhibit superconducting behavior any more.

Independently, the author[25,26] reported the appearence of a dc voltage in the superconducting film of a tunnel junction for high tunnel current exceeding a certain critical value with the configurations given in Fig. 1. This critical tunnel current lies far below the critical current of the superconducting film itself and typically ranges between 10^2 and 10^3 A/cm^2. He also observed that the critical current of the superconducting film decreased with increase of tunnel current. In a recent letter,[27] this phenomenon was identified as a result of large quasiparticle injection by an external current source and was a characteristic of the nonequilibrium state of superconductors. With

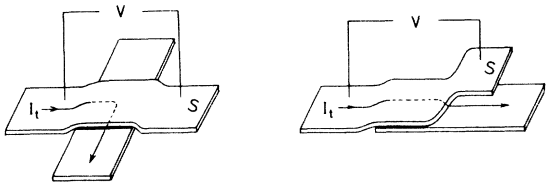

(a) (b)

FIG. 1. Schematic representation of the thin-film geometries for (a) cross-type junction and (b) linear-type junction where I_t is a tunnel current and V is a generated voltage in the film.

the same terminal pick-up configuration, Gundlach[28] observed the same phenomenon using narrower strips. A similar phenomenon has been also reported by Hebard.[29]

Owen and Scalapino[30] first proposed a theoretical model for superconductors in the nonequilibrium state based on the BCS theory. In this model, it is assumed that the artificially injected quasiparticles are in thermal equilibrium with the phonons at the lattice temperature T with their distribution displaced by an effective chemical potential μ^*. The system is considered to be in thermal equilibrium but not in chemical equilibrium with the pairs. The μ^* model predicts a decrease of the gap parameter with increase of the excess quasiparticle density and a first-order transition to the normal state. Although the former result was confirmed experimentally,[3,4] the latter one, as stated above, has not yet been observed by the photoinjection experiments. Chang and Scalapino[31] attributed the absence of a first-order transition to the presence of an instability due to long-range quasiparticle density fluctuations.

On the other hand, Parker[32] has recently proposed a modified heating model in which the recombination phonons play an important role for creation of quasiparticles rather than escape from the superconductor. The system here is assumed to be characterized by a certain effective temperature T^* at which the quasiparticles and the phonons with energy greater than 2Δ are in quasiequilibrium, where Δ is the gap parameter. Since this T^* model is based on the equilibrium properties of superconductors, the absence of a first-order transition causes no trouble. The effective gap decreases with increasing excess quasiparticle number density.

For small quasiparticle injection rate, both models explain the experimental results quite well. For large injection rate, however, there is a substantial discrepancy between these two. Experimentally, there appears an intermediate dc resistance state which cannot be expected from these models describing a spatially homogeneous state, indicating the presence of a spatially inhomogeneous state.[4,5,7,31,33]

It is the purpose of this paper to describe the phenomenon observed in superconducting tunnel junctions under the influence of a large tunnel current in Refs. 25–27 in detail and to provide some insight for the understanding of the real situation occurring in the nonequilibrium state of superconductors by comparing the experimental data with the theories. It is also the purpose to show that our observations and those by Wong, Yeh, and Langenberg[24] are essentially the same and that they can be reasonably interpreted using the quasiparticle injection model. Most of the experimental results given here were presented at the Japan Physical Society meetings in 1975 and 1976.

In Sec. II, a theory based on the modified Rothwarf-Taylor equations and the T^* model is formulated. The analysis for the four-terminal measurement is important in connecting the experimental data with the theory and is also given here. Section III describes the experimental details, while Sec. IV is devoted to the experimental results and their discussion in terms of the quasiparticle injection model. Section V contains our conclusions.

II. THEORETICAL APPROACHES

A. Nonequilibrium model

We use the rate equations of Rothwarf and Taylor[34] for quasiparticle injection from a current source, but in a modified fashion. The Rothwarf-Taylor equations do not take the energy distribution of quasiparticles into account. In our experiments quasiparticles are, however, mostly injected through a tunnel barrier at high bias voltages (10–50 mV) $\gg \Delta$. We include this effect in the following way. The quasiparticles injected at high voltages relax toward the gap edge by the emission of phonons. At a bias voltage V_t, the average energy of the injected quasiparticles is approximately given by $\frac{1}{2}(V_t+\Delta)$ since the tunnel resistance is almost constant for $V_t \gg \Delta$. In the relaxation process, on the average, they lose energy $\frac{1}{2}(V_t+\Delta)-\epsilon$ ($\epsilon \geq \Delta$). We consider that one injected quasiparticle eventually creates by recombination approximately $F(V_t+\Delta-2\epsilon)/2\hbar\omega$ phonons with energy $\hbar\omega \geq 2\Delta$, where F is the fraction of the energy converted to quasiparticles[32,35] and is related to the phonon density of states in superconducting materials. For example, $F \simeq \frac{2}{3}$ for Pb and $F \simeq \frac{3}{4}$ for Sn.[35] With the assumption of $\epsilon = \Delta$ and $\hbar\omega = 2\Delta$,[36] $FI_0(V_t-\Delta)/4\Delta$ phonons are produced for quasiparticle injection rate I_0 ($\sec^{-1}\mathrm{cm}^{-3}$).

These phonons also act on the pair breaking. Then the modified rate equations become

$$\frac{dN}{dt} = I_0 + \frac{2N_\omega}{\tau_B} - \kappa N^2 \tag{1}$$

and

$$\frac{dN_\omega}{dt} = \frac{F(V_t - \Delta)}{4\Delta} I_0 + \frac{\kappa N^2}{2} - \frac{N_\omega}{\tau_B} - \frac{N_\omega - N_{\omega T}}{\tau_\gamma}, \tag{2}$$

where N is the number density of quasiparticles, N_T is the thermal equilibrium number density of quasiparticles, N_ω is the number density of phonons with $\hbar\omega \geq 2\Delta$, $N_{\omega T}$ is the thermal equilibrium number density of phonons with $\hbar\omega \geq 2\Delta$, κ is a recombination coefficient, τ_B is the mean rate at which phonons with $\hbar\omega \geq 2\Delta$ create quasiparticles, and τ_γ is the net transition probability for loss of phonons from the energy range $\hbar\omega \geq 2\Delta$ through processes other than pair breaking. Near T_c the number of phonons with the energy 2Δ decreases to zero as $T \to T_c$ because the density of states decreases as ω^2 for low-energy phonons.[37] Hence Eq. (2) is not a good approximation near T_c. It has been also pointed out[37,38] that the inelastic scattering time is longer than the recombination time in a substantial region of energies and temperatures. In this case we may probably take $\epsilon \simeq \Delta_0$ for all temperatures. In the steady state, $dN/dt = dN_\omega/dt = 0$ and we have the solutions

$$N_\omega = N_{\omega T} + \tfrac{1}{2} I_0 \tau_\gamma f \tag{3}$$

and

$$N^2 = N_T^2 + (I_0/\kappa)[1 + (\tau_\gamma/\tau_B) f], \tag{4}$$

where $f \equiv 1 + F(V_t - \Delta)/2\Delta$. In the no-injection limit, the relation $\kappa\tau_B = 2N_{\omega T}/N_T^2$ is derived. In the phonon-trapping regime $\tau_\gamma \gg \tau_B$, the excess phonon number density becomes almost the same order of magnitude as the excess quasiparticle number density for large injection.

Let us consider Parker's T^* model[32] here because the experimental results mostly show a second-order transition of superconductors in our experimental temperature range 1.9–4.2 K. When $\tau_\gamma \gg \tau_B$, the phonons are substantially out of equilibrium. In this case Eqs. (3) and (4) yield the relation $(N/N_T)^2 \simeq N_\omega/N_{\omega T}$. It is assumed in this model that the quasiparticles and the phonons with energy $\hbar\omega \geq 2\Delta$ are in quasiequilibrium at an elevated temperature T^* different from the bath temperature T, while the phonons with energy $\hbar\omega < 2\Delta$ are characterized by the bath temperature T. Then, using a Debye model for the phonon density of states, we obtain

$$\left(\frac{N}{N_T}\right)^2 \simeq \left(\frac{T^*}{T}\right)^3 \int_{2\Delta(T^*)/k_B T^*}^{\infty} \frac{x^2 dx}{e^x - 1} \times \left(\int_{2\Delta(T)/k_B T}^{\infty} \frac{x^2 dx}{e^x - 1} \right)^{-1}, \tag{5}$$

where $\Delta(T)$ and $\Delta(T^*)$ are the temperature-dependent gap parameters. The superconducting properties of this system are described by a BCS superconductor at the elevated temperature T^*. We simply assume the relation between the tunnel current density J and the injection rate I_0 as $I_0 = J/ed$, where d is the film thickness and e is the electron charge, since one electron through a tunnel barrier creates one quasiparticle for each film. Then, by substituting the N of Eq. (4) into Eq. (5), we obtain

$$J \simeq (2ed/f\tau_\gamma)(N_{\omega T^*} - N_{\omega T}). \tag{6}$$

When $V_t \gg \Delta$, $f \simeq FV_t/2\Delta$. With the assumption $V_t \simeq I_t R_n$, where R_n is the tunnel resistance in the normal state, Eq. (6) becomes

$$J \simeq \left[\frac{2ed\Delta}{\pi^2 F \rho_n \tau_\gamma} \left(\frac{k_B}{\hbar c_s} \right)^3 \times \left(T^{*3} \int_{2\Delta(T^*)/k_B T^*}^{\infty} \frac{x^2 dx}{e^x - 1} - T^3 \int_{2\Delta(T)/k_B T}^{\infty} \frac{x^2 dx}{e^x - 1} \right) \right]^{1/2}, \tag{7}$$

where c_s is the averaged sound velocity and $\rho_n \equiv R_n A$ with A the junction area. The critical tunnel current density at $T = 0$ is obtained from Eq. (7) simply by setting $T \to 0$ and $T^* = T_c$. The result is

$$J_c(0) \simeq \left[\frac{4\zeta(3) ed\Delta_0}{\pi^2 F \rho_n \tau_\gamma} \left(\frac{k_B T_c}{\hbar c_s} \right)^3 \right]^{1/2}, \tag{8}$$

where $\zeta(3) = 1.202\cdots$. The critical current density at finite temperatures is also calculated from Eq. (7). $J_c(T)$ almost reaches $0.95 J_c(0)$ at $T/T_c = 0.6$.

In a good approximation, it is shown[21,35,39] that $\tau_\gamma \simeq 4d/\eta c_s$, where η is the average phonon-transmission probability at the film interface. If this relation is used, $J_c(T)$ depends only on η and is independent of d in the T^* model. As an example, for tin at $T = 2$ K, using the values $c_s = 2 \times 10^5$ cm/sec, $\Delta = 0.56$ mV, $\eta \simeq 0.5$ for superfluid helium[40] and $\rho_n \simeq 10^{-4}\ \Omega\ \text{cm}^2$, we obtain $J_c(2K) \simeq 4.7 \times 10^2$ A/cm^2.[41] Note that the above relation holds when the phonon mean free path λ against pair breaking is larger than d. In our experiments, probably $\lambda \sim d$.

When T^* exceeds T_c but T remains below T_c, the normal-state properties of a metal will be almost identical to that of the metal in thermal equilibrium at the temperature T^*.[42] If we assume that the $J - T^*$ relation in Eq. (7) also holds beyond

$T^* = T_c$, we should expect $J \propto T^{*1.5}$ at the low bath temperatures. Then the resistivity due to the inelastic phonon scattering becomes proportional to T^{*5}, hence to $J^{3.3}$. The resistive behavior in current-voltage characteristics followed by the film transition, however, depends on the actual film condition (i.e., impurity contamination).

In the above treatment we neglected the effect of quasiparticle diffusion. For a tunnel junction geometry, it may be possible that the quasiparticles which are injected into the restricted area of a superconducting film diffused from the junction edge. But it was found experimentally that the quasiparticle diffusion was quite small when the injection rate was high (see Sec. IV F).

It is instructive here to compare the tunnel critical current I_{tc} with the film critical current I_c. The critical current of a superconducting film by the free energy criterion is given by[43,44]

$$I_c = [cH_0 w_1 d/4\pi\lambda_L(0)][1-(T/T_c)^2]^{3/2}, \tag{9}$$

where H_0 is the bulk critical field at $T=0$, $\lambda_L(0)$ is the London penetration depth at $T=0$, w_1 is the film width, and c is the velocity of light. On the other hand, the order of I_{tc} has been estimated in Ref. 27 and for low temperatures

$$I_{tc} \sim 2edw_1 w_2 N(0)\Delta_0/\tau_{eff}, \tag{10}$$

where w_2 corresponds to the width of a crossing film for cross type junctions and to the intrusion length of the other film to the junction area for linear-type junctions (see Fig. 1). τ_{eff} is the characteristic quasiparticle relaxation time given by

$$\tau_{eff} = \frac{2N_T}{\delta N + 2N_T}\,\tau_R\left(1+\frac{\tau_\gamma}{\tau_B}f\right), \tag{11}$$

with

$$\delta N \equiv N - N_T = \tfrac{1}{2} I_0 \tau_{eff}, \tag{12}$$

where δN is the excess quasiparticle number density and $\tau_R = 1/\kappa N_T$ is the intrinsic recombination time. The current ratio for Pb at $T=0$, using the values $H_0 \simeq 800$ G, $\lambda_L(0) \simeq 370$ Å, and $N(0)\Delta_0 = 2.47 \times 10^{19}$ cm^{-3},[18] becomes $(I_{tc}/I_c)_{T=0} \simeq 4.6 \times 10^{-8} w_2/\tau^0_{eff}$ where w_2 is in cm and τ^0_{eff} in sec. It is noted that the ratio I_{tc}/I_c is proportional to w_2. Taking $\tau^0_{eff} \sim 2 \times 10^{-8}$ sec and $w_2 = 0.01$ cm, we find 2.3×10^{-2} for the ratio. With the above expression, the quasiparticle relaxation time is delayed considerably for high-energy quasiparticles owing to the factor f.

B. Four-terminal problem

The current-voltage characteristics of a junction are measured by the four-terminal method. Pedersen and Vernon[45] and Giaever[46] investigated this problem with the spatial variation of a current flow in a junction taken into account. We follow their simple treatment here and calculate the quantities for our special terminal pick-up in one dimension (see Fig. 1). We assume that, for the finite voltage state of a film, the resistance is distributed uniformly in the film at the junction, although it may be allowed to depend generally on the magnitude of a tunnel current. This assumption is reasonable for the normal film, but will be certainly invalid for the treatment of a spatially inhomogeneous intermediate state of superconductors. Nevertheless, we may consider that the averaged gross behavior of current-voltage characteristics will be described by this approach.

Now consider a geometrical tunnel current flow as illustrated in Fig. 2. If $I_1(x)$ and $I_2(x)$ are the currents in the film 1 and 2, respectively, and $V_t(x)$ is the potential drop across the junction at a position x, the following equations hold:

$$\frac{\partial V_t}{\partial x} = r_2 I_2 - r_1 I_1, \tag{13}$$

$$\frac{\partial I_1}{\partial x} = -gV_t = -\frac{\partial I_2}{\partial x}, \tag{14}$$

where r_1 and r_2 are the resistances per unit length of films 1 and 2, respectively, and g is the junction conductance per unit length. The length of the junction is l. The tunnel current $I_t = I_1 + I_2$ is independent of x. The solution of Eqs. (13) and (14) is obtained under the appropriate boundary conditions and the result is

$$V_t(x) = (I_t/\alpha l \sinh\alpha l) \times [R_1 \cosh\alpha(x-l) + R_2 \cosh\alpha x], \tag{15}$$

where $R_1 \equiv r_1 l$, $R_2 \equiv r_2 l$, and $(\alpha l)^2 \equiv g(r_1+r_2)l^2 = (R_1 + R_2)/R_t$, with R_t the tunnel resistance. Using the above solution, we obtain the same expression for the measured tunnel resistance as in Ref. 45. For $\alpha l \ll 1$, which is the usual situation for our samples in spite of their low tunnel resistances, the tunnel

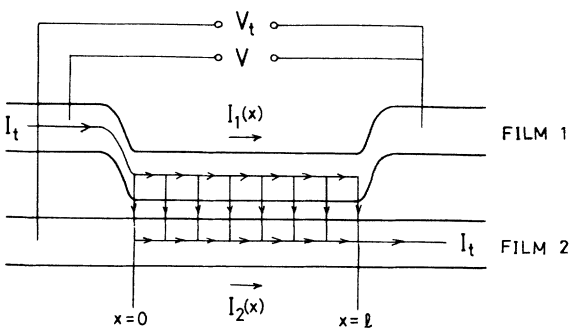

FIG. 2. Schematic illustration of a tunnel current flow in a junction for the four-terminal analysis.

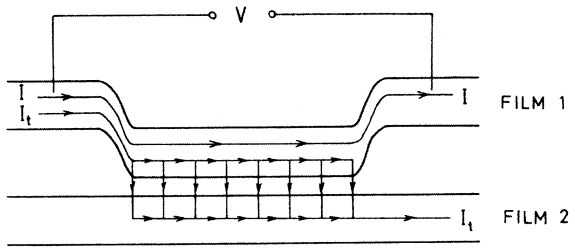

FIG. 3. Schematic illustration of a tunnel current flow in a junction under the influence of a transport current I in the film.

voltage V_t is approximately given by

$$V_t \simeq R_t I_t\left[1-\tfrac{1}{6}(R_1+R_2)/R_t+\cdots\right]. \tag{16}$$

In our measurements, the voltage V in Fig. 2 is also measured. The expression for V is given by

$$V=\frac{R_1 R_2}{R_1+R_2} I_t\left[1-\left(1-\frac{R_1}{R_2}\right)\frac{\tanh\frac{1}{2}\alpha l}{\alpha l}\right]. \tag{17}$$

For $\alpha l \ll 1$, we have

$$V \simeq \frac{R_1}{2} I_t\left[1+\frac{1}{12}\left(1-\frac{R_1}{R_2}\right)\frac{R_2}{R_t}+\cdots\right] \simeq \frac{R_1}{2} I_t . \tag{18}$$

It is important to note that $V=0$ when $R_1=0$. Therefore the detection of any finite voltage in a superconducting film indicates the appearance of a nonsuperconducting state in it at least partially. Differentiation of V with respect to I_t yields, in the limit of $\alpha l \to 0$,

$$\frac{dV}{dI_t} \simeq \frac{R_1}{2}+\frac{I_t}{2}\frac{dR_1}{dI_t} \tag{19}$$

for the superconducting (film 1)-insulator-normal (film 2) junctions. While R_1 is generally a function of I_t, R_2 is not. The change in R_t for $V_t \gg \Delta$ produces only a small effect according to Eq. (18). Since Eq. (19) contains the term dR_1/dI_t, we expect a peak structure in the dV/dI_t curve whenever R_1 changes step-function-like with I_t. This behavior is seen in Fig. 8.

If there exists another independent current I through the film 1 as shown in Fig. 3, then the result is modified to give for $\alpha l \ll 1$,

$$V \simeq R_1(\tfrac{1}{2}I_t+I). \tag{20}$$

When I_t and I are antiparallel, the I_t-vs-V characteristic for a fixed value of $I=I_B$ extends to a negative voltage region provided that $|I_t|<2|I_B|$. On the other hand, when I_t and I are parallel, the voltage V develops more rapidly than the case of $I_B=0$ with an increase of I_t. This behavior is also seen in Fig. 15.

It is more instructive to discuss these characteristics in terms of the differential forms. By differentiating Eq. (20) with respect to I, we have

$$\frac{\partial V}{\partial I} \simeq R_1 . \tag{21}$$

Here R_1 was assumed to be independent of I. This assumption is reasonable when the current-voltage characteristic of the film in the resistive state is ohmic. Relation (21) is important because it gives the actual variation of the film resistance R_1 with I_t. Experimentally the R_1-vs-I_t curve is obtained by fixing I_t at a certain value and establishing a small ac current δI along the film. Differentiation of V with respect to I_t yields the result

$$\frac{\partial V}{\partial I_t} \simeq \frac{R_1}{2}+\left(\frac{I_t}{2}+I\right)\frac{\partial R_1}{\partial I_t}. \tag{22}$$

Note that, with the above formulation, the roles of I and I_t are clearly separable.

The spatial distribution of the tunnel current density in the junction is given by $J(x)=gV_t(x)$. While the film 1 is wholly superconducting (i.e., $r_1=0$), $J(x)$ takes the maximum value at $x=l$. When this maximum current density equals J_c, the film starts to make a transition to the normal state. Therefore the experimentally observed value is connected with the calculated one by the relation

$$J_c^{\text{expt}} = J_c^{\text{theor}} \tanh\gamma l/\gamma l , \tag{23}$$

where $\gamma l \equiv (R_2/R_t)^{1/2}$. In most samples, however, $\gamma l \ll 1$ and $J_c^{\text{expt}} \simeq J_c^{\text{theor}}$. When both films are superconducting and identical, $J_c^{\text{expt}} = J_c^{\text{theor}}$.

III. EXPERIMENTAL PROCEDURES

The samples were prepared by first evaporating a metal onto either a glass or sapphire substrate utilizing thin stainless-steel masks, then allowing it to oxidize, and finally evaporating a metal counter electrode. Typical film thicknesses are 1000 to 2000 Å and the widths are 20 to 200 μm. In this experiment it is necessary to make a junction with low tunnel resistance (10^{-4}–10^{-5} $\Omega\,\text{cm}^2$) in order to allow high tunnel current density. As for the oxidation of Pb and Sn, we followed the usual methods reported elsewhere. Whenever a NiCr-Cu film is used as a normal film, we evaporate Cu (~2000 Å) and NiCr (~200 Å) subsequently and oxidize the surface of the NiCr film by exposing the sample in a wet atmosphere for a few days. The oxide layer formed in this way was found to be quite uniform and reliable. We fabricated both *S-I-N* (superconducting-insulator-normal) and *S-I-S* (superconducting-insulator-superconducting) -type junctions. Each end of the film has two independent silver contact areas at which Cu leads are connected using indium solder.

To obtain the various characteristics of a junc-

tion, a triangle wave of frequency 0.1–0.0001 Hz from a generator was used as a low-speed current sweeper. The first derivative measurements of characteristics were done by modulating the applied dc bias current with a small constant-current ac signal and picking up the generated voltage in the junction section with a lock-in amplifier. The modulating frequencies were chosen at 430 and 470 Hz. The second derivative measurements were done by detecting the second harmonic of the applied dc modulation using a lock-in amplifier.

The normal-state properties of a superconducting film were determined by applying an external magnetic field perpendicular to the film surface. The junction evaluation was done by measuring its energy gap. For Pb-*I*-NiCr-Cu junctions, the value of the measured gap parameter was $\Delta_{expt} = 1.27 \pm 0.02$ mV at $T = 4.2$ K. All data were taken with the samples immersed in liquid helium. For incomplete junctions such as those having pinholes, a similar kind of effect was also observed, which is probably correlated with the idea of "point injection" given in Ref. 24.

IV. EXPERIMENTAL RESULTS AND DISCUSSION

A. I_t-V characteristic and critical tunnel current

In Fig. 4, we show the typical I_t-V characteristic of a lead junction together with its tunneling characteristic. There is apparently no corresponding change in the tunneling characteristic at the threshold of the appearance of a dc voltage in the superconducting film. As shown in Fig. 8, however, there is actually a small change in its derivative characteristic. The voltage develops nonlinearly and never approaches ohmic behavior. This qualitative structure is observed in both cross- and linear-type junctions (see Fig. 1). In cross-type junctions, the current flow divided to the other crossing film yielded the same result as that given in one direction only. These results indicate that the bending of current flow is unimportant for the occurrence of the effect. There is almost no hysteresis in both the I_t-V and the tunneling characteristics up to higher currents. Although the qualitative features are similar for glass and sapphire substrates, the detailed I_t-V characteristic is different between these two. The phonon transmission probability at the metal-sapphire interface is much greater than that at the metal-glass interface. Hence, when a sapphire substrate is used, larger injected power is necessary for observing a dc voltage [see Eq. (6)]. As a result, a broad transition region is observed (Sec. IV C). There is only little change in the I_t-V characteristic in passing through the λ temperature. On the other hand, when a glass substrate is used, the phonon trapping effect is strong. Therefore, just below T_λ, the critical tunnel current I_{tc} at which a dc voltage appears in the superconducting film increases rapidly but continuously owing to the enhancement of η in superfluid helium.

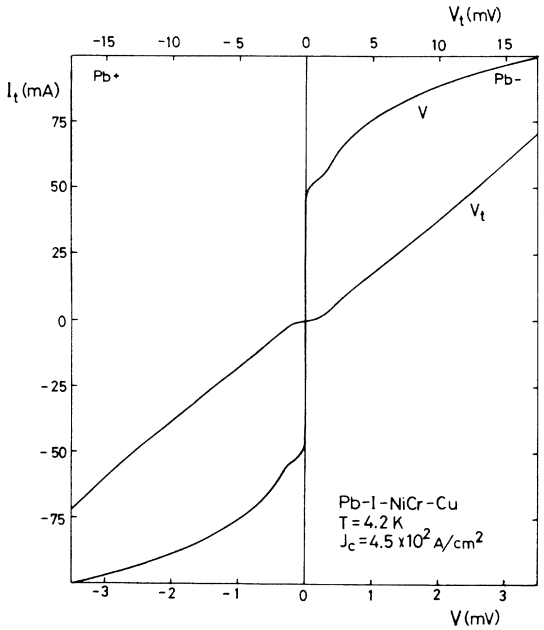

FIG. 4. I_t-V characteristic and the tunneling characteristic for a Pb-*I*-NiCr-Cu junction.

For bath temperatures below T_λ, we have frequently observed a jump at the threshold corresponding to a first order transition of the superconducting film. If the sample is covered by thin photoresist film, this effect was suppressed, also indicating that the phenomenon is closely related to phonon-escape mechanism from the sample surface.

In the case of tin junctions, although the threshold behavior is similar to that of lead junctions, their characteristics are often accompanied by several jumps for higher currents.

The critical tunnel-current density J_c (I_{tc} divided by junction area) is generally 10^2–10^3 A/cm^2 for samples with junction area 10^{-5}–10^{-3} cm^2 at temperatures well below T_c. It depends on the superconducting materials and their conditions. For Sn-*I*-*N* junctions on glass substrate at $T = 2.0$ K, J_c ranges from 3×10^2 to 7×10^2 A/cm^2, while the theoretical estimate based on the T^* model with $\eta = 0.5$ and $\rho_n \simeq 10^{-4}$ Ω cm^2 yields $J_c(2\text{ K}) \simeq 4.7 \times 10^2$ A/cm^2, in good agreement with the experimental values. For Pb-*I*-*N* (or *S*) junctions, the theoretical estimate also yields almost the same order of magnitude as the experimental ones. The temperature dependence of J_c was studied using tin junctions. J_c increases with decreasing bath tem-

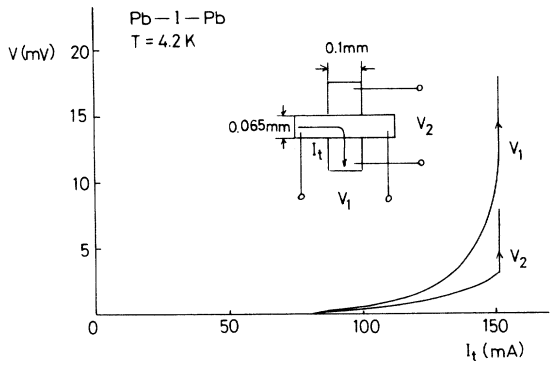

FIG. 5. I_t-V characteristics for a Pb-I-Pb junction. The onset of a voltage occurs almost at the same point for both films. The jumps are probably associated with thermal instability.

perature and shows a saturating behavior at about $T/T_c = 0.6$.[27] Whenever several junctions with different areas were fabricated on the same substrate simultaneously, we always observed almost the same values of J_c irrespective of their areas, supporting the idea of quasiparticle injection.

In the case of S-I-S junctions, the quasiparticles are injected into both superconducting films and voltages appear in them unless they are in Josephson coupling. If both films are identical, both J_c's coincide regardless of their widths. In Fig. 5, we show an example for Pb-I-Pb junction. The observed jumps at $I_t = 150$ mA are probably associated with thermal instability.

B. Gap suppression

For the behavior below J_c (or I_{tc}), although no appreciable voltage appears in the film, the effective gap is expected to decrease with an increase of I_t on account of quasiparticle injection. It was observed that the critical current of the superconducting film decreased with increasing bias tunnel current I_t (Fig. 6). It is noticeable that there is very little change in the critical current below $I_t \simeq 27$ mA. This behavior was previously studied in Refs. 25 and 26, and also intensively studied by Wong, Yeh, and Langenberg[24] in connection with the making of weak links.

To study the effective gap decrease by injection current directly, we have performed the experiment utilizing the N-I-Pb-I-N-type double-tunnel-junction as illustrated in Fig. 7. The quasiparticles are injected through the upper tunnel junction, while the lower one constitutes a gap detector of the middle superconducting film. We see that the effective gap decreases continuously with increasing injection current. With the geometrical configuration shown in Fig. 7, however, only the spatially averaged gap suppression can be studied since the quasiparticles are injected into a part of a detecting area of the middle film. The junction conductance increases very slowly below $\sim 0.4 I_{tc}$ whose behavior is consistent with the results in Fig. 6. For $I_t \gtrsim 0.4 I_{tc}$, it rises up and reaches nearly 60% of normal conductance value at $I_t = I_{tc}$. For further increase of the tunnel current, it approaches the full normal value. We may approximately evaluate the effective gap from the experimental data and find that it actually becomes zero at about the end of the transition region (Sec. IV C). The results are close to the theoretical curve obtained from the T^* model only for the regions near $I_t = 0$ and $I_t = I_{tc}$ but deviate from it in the broad range of injection current. In addition, below T_λ, a first order transition was sometimes observed with this geometry.

C. Differential characteristics

Figure 8 shows the various derivative characteristics of a junction with respect to a tunnel current I_t. All three curves were taken simultaneously for the identical sample. The upper curve is the derivative of the voltage V in the superconducting film, while the lower one corresponds to that in the normal film. The middle one exhibits the differential tunneling characteristic.

The peak observed just after the threshold in the upper curve corresponds to the transition of a superconducting film to the normal state. This behavior can be expected from Eq. (19), if the local film resistance R_1 which is a part of the tunnel junction varies like a smeared step function with

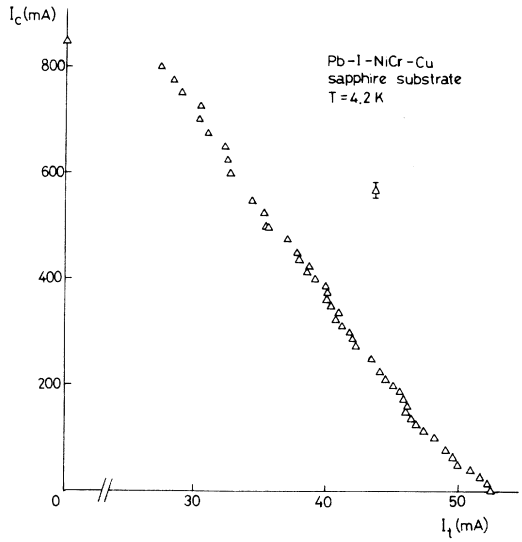

FIG. 6. Critical current of a superconducting film under the influence of bias tunnel current I_t.

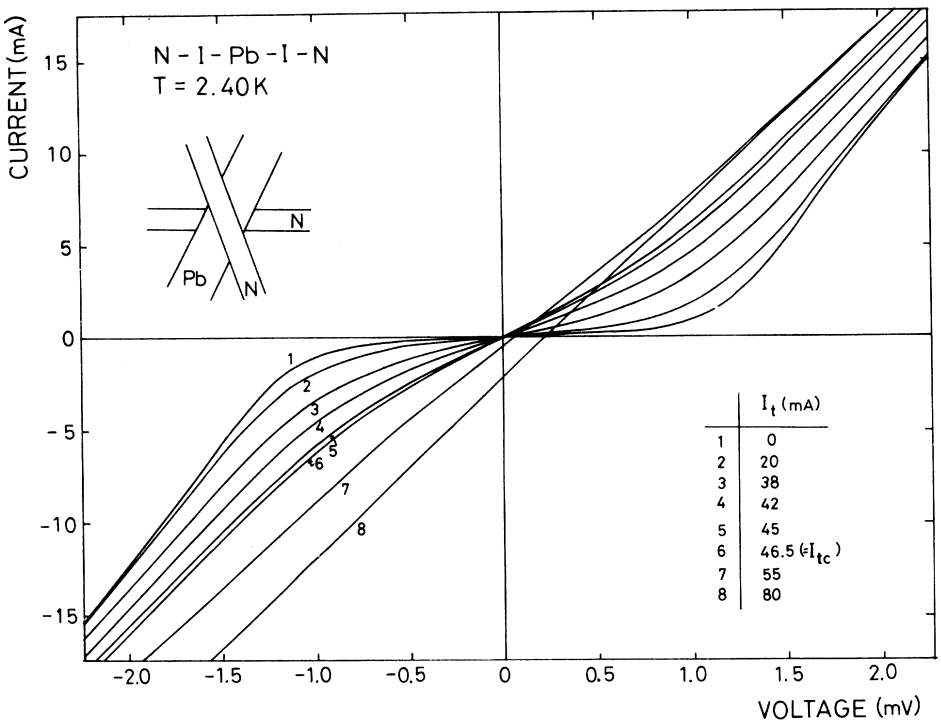

FIG. 7. Variation of the tunneling characteristic with injection current I_t for a double-tunnel-junction geometry.

I_t. It is shown later that this is indeed true (see Fig. 9). The total width of the transition region is generally $\lesssim 0.4I_{tc}$ for the samples with glass substrates, whereas it is $\sim 0.8I_{tc}$ for those with sapphire substrates. There is a clear tendency for the width of the transition region at a given temperature to become broader as the power injected per unit area at $I_t = I_{tc}$ increases. For example, it is $\sim 0.1I_{tc}$ for injector power 0.5 W/cm^2 and $\sim 0.8I_{tc}$ for injector power 7 W/cm^2. In order to compare our results with the intermediate dc resistance region observed in laser experiments,[4,5] it is necessary to interpret our observed width in terms of the injector power P which corresponds to laser light intensity and is approximately proportional to $R_n I_t^2$ rather than I_t itself. Then, by defining P_c as the critical injector power at $I_t = I_{tc}$, we obtain the corresponding width as $\sim 2P_c$ for the case of a sapphire substrate, which result is consistent with the observations by laser light, and $\lesssim P_c$ for the case of a glass substrate. In the case of a sapphire substrate, the phonon transmission into the substrate side is large, hence P_c is large according to Eq. (6). When the absorbed power in steady state is large, the system is strongly perturbed, which will produce the broad intermediate dc resistance state consisting of the spatially distributed superconducting and normal regions. The intermediate state is relatively narrow for the case of a glass substrate. When the absorbed power is very small, the intermediate state almost vanishes. In this case, we consider that quasiparticles will be described by some type of thermal-equilibrium distribution.

The differential characteristic in the normal film contains the contributions from both the junction part and electrode part outside the junction region. They are separable and the expected magnitude of the film resistance for the junction part is indicated by a bar in Fig. 8. It is found that there exists almost no change in the normal film corresponding to the threshold behavior in the superconducting film, suggesting that the phenomenon is characteristic to the superconducting state. A dip seen around the origin is due to the large change of the tunnel resistance below the gap edge.

In the differential tunneling characteristic, the wavy structure near the gap edge is typical for strong coupling Pb, while the continuous increase of conductance is probably due to the inelastic phonon effect in an oxide layer. There is, however, a dip corresponding to the threshold peak in the upper curve. This behavior can be simply interpreted as a result of the four-terminal measurement in the following way. From Eq. (16) the measured differential tunnel resistance becomes

$$\frac{dV_t}{dI_t} \simeq \left(R_t - \frac{R_1 + R_2}{6}\right) - \frac{I_t}{6}\frac{dR_1}{dI_t},$$

where both R_t and R_2 are assumed to be indepen-

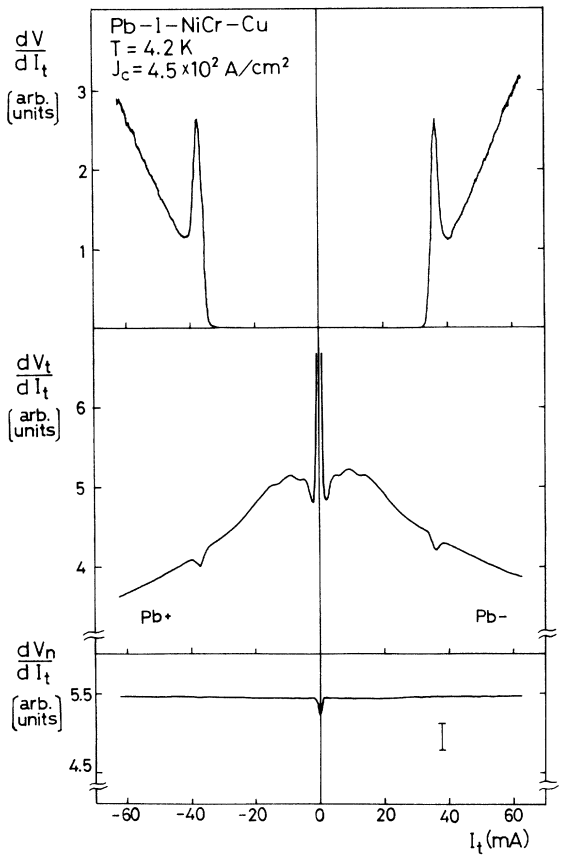

FIG. 8. Differential characteristics for an identical junction. The upper curve represents the dV/dI_t characteristic in the superconducting Pb film, the middle one represents the first derivative of the tunneling characteristic, and the lower one represents the dV/dI_t-I_t characteristic in the counter normal film. The modulating *ac* current amplitude is 0.5 mA and time constant is 1 sec.

dent of I_t since R_t is almost constant for $V_t \gg \Delta$ and R_2 here is the normal film resistance. On the other hand, for dV/dI_t, we have relation (19). In both equations a local peak or dip is represented by the dR_1/dI_t term. Therefore, by extracting the background gross structure, we obtain the simple relationship

$$\left(\frac{dV_t}{dI_t}\right)_{\text{dip}} \Big/ \left(\frac{dV}{dI_t}\right)_{\text{peak}} \simeq -\frac{1}{3}.$$

The observed ratio almost yielded this value for the junctions with $\alpha l \ll 1$. It is important to note that while the change in R_1 affects dV_t/dI_t appreciably, the change in R_t affects dV/dI_t very little according to Eqs. (16) and (18) for $\alpha l \ll 1$.

The dependence of the film resistance R_1 of the junction part on a given I_t can be measured, according to Eq. (21), by feeding a fixed dc current I_t and a small ac current signal δI as shown in Fig. 3, then detecting the modulating signal using a lock-in amplifier. Such results are shown in Fig. 9. The value of R_1 indicated by an arrow in the figure corresponds to the expected film resistance of the junction part when the film is in the normal state under the influence of an external magnetic field. Just after I_{tc}, R_1 varies indeed smeared-step-function-like with I_t, showing the broad transition of a superconducting film. For higher values of I_t, R_1 behaves as I_t^ν apart from its origin with $1 \leq \nu < 2$ for the samples with glass substrates and $\nu \simeq 1$ for those with sapphire substrates. If we consider that this behavior arises from the inelastic scattering by the phonons in steady state, we expect the larger value of ν for glass substrates than for sapphire substrates since phonons are less trapped for the latter. R_1 is independent of I_t for the μ^* model. For the T^* model, the actual temperature dependence of the resistance for each film is necessary to calculate the value of ν.

Figure 10 shows the second derivative characteristic d^2V_t/dI_t^2 against the tunnel voltage V_t both with and without an external magnetic field. In the curve with no magnetic field, the first two peaks nearer the gap edge correspond to transverse and longitudinal phonons respectively. The observed phonon energies measured from the gap edge are $\hbar\omega_T = 4.2 \pm 0.2$ mV for the transverse phonon and $\hbar\omega_L = 8.2 \pm 0.2$ mV for the longitudinal phonon, in good agreement with the previous measurements.[47-51] There are a phonon harmonic structures in the medium voltage region and a large change corresponding to the dip in dV_t/dI_t curve

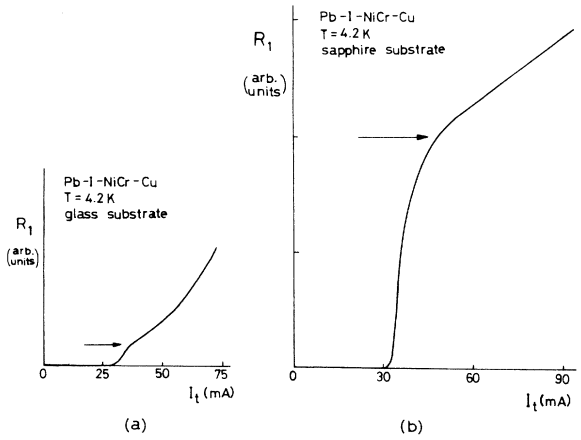

FIG. 9. Dependence of the film resistance R_1 of the junction part on I_t for (a) the sample with a glass substrate and (b) the sample with a sapphire substrate. The arrows in the figures indicate the expected normal state resistances of the junction part obtained from independent measurements in a magnetic field.

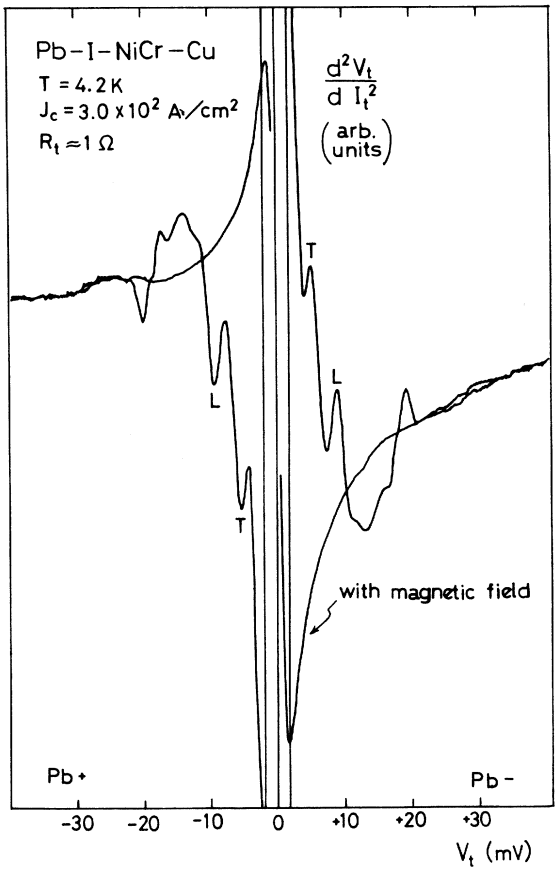

FIG. 10. Second derivative d^2V_t/dI_t^2 of the tunneling characteristic with and without an external magnetic field. L and T correspond to the transverse and longitudinal phonon peaks, respectively.

of Fig. 8 around $V_t = 20$ mV. After this change, the curve exactly coincides with the normal state curve with magnetic field, showing that the film actually enters into the normal state or a nonsuperconducting nonequilibrium state. This situation is discussed in next paragraph. In the dV_t/dI_t curve, the same behavior was also seen under the influence of a magnetic field.

D. Against simple heating

Although the dissipated power is small at temperatures well below T_c (0.5–5 W/cm²), it is still important to test the possibility of simple heating effect.[52] The absence of hysteresis and thermal instability in both the I_t-V and the junction tunneling characteristics at least supports the minor involvement of simple heating effect even above T_λ. The I_t-V characteristic responded to 10-μsec pulses. It is also understood from Fig. 8 that while a drastic change is observed in the superconducting film, no appreciable change is seen in

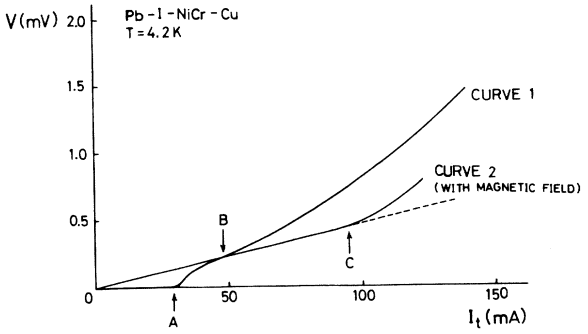

FIG. 11. I_t-V characteristics of the junction part with (curve 2) and without (curve 1) an external magnetic field. A is the point of voltage onset, B is the point at which the generated voltages for both curves becomes equal, and C is the point about which the curve 2 deviates from an Ohmic behavior.

the counter normal film. This fact excludes the possibility of a simple heating effect because both films must be heated in this case and some change in the normal film is also expected. The more direct way to investigate this problem is given in the following way. In Fig. 11, we took the I_t-V characteristic for a Pb-I-NiCr-Cu junction on a sapphire substrate (curve 1). Applying a magnetic field, we can also take the same characteristic in the normal

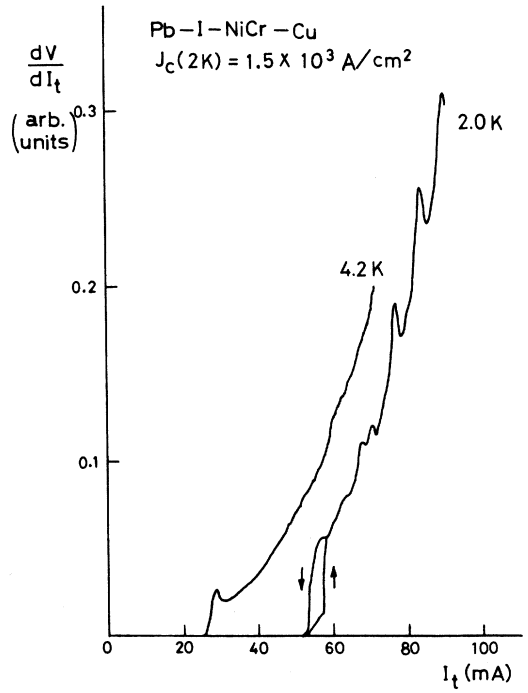

FIG. 12. dV/dI_t characteristics at $T = 4.2$ K and $T = 2.0$ K for a Pb-I-NiCr-Cu junction with a glass substrate. Note that there appears a sequence of small peaks in the characteristic at $T = 2.0$ K.

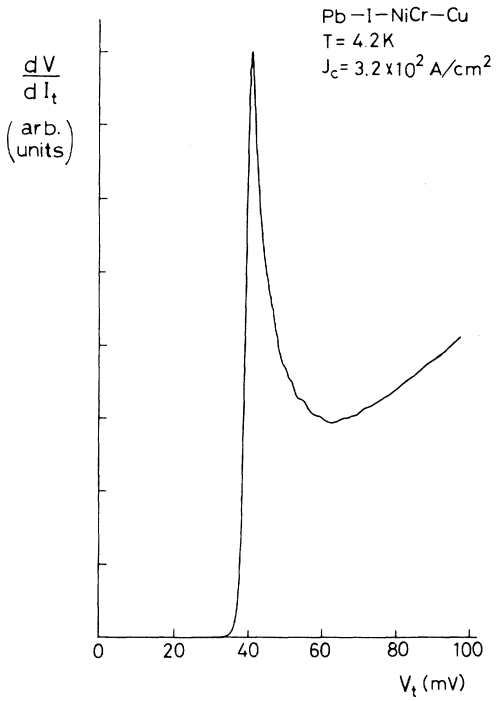

FIG. 13. dV/dI_t-I_t characteristic at $T = 4.2$ K for a Pb-I-NiCr-Cu junction with a sapphire substrate. A nearly periodic wavy structure can be seen in the figure.

state, but the data contain the contributions from both the junction part and the electrode part outside the junction region. We can separate these contributions by including the nonlinear effect into the junction part and the expected behavior of the junction part is shown by curve 2. In discussing the curve 1, the film starts to enter into a nonequilibrium resistive state at point A and this state at least lasts, through point B at which the film recovers the full value of its resistance, to point C about which a nonlinear behavior is observed even for the film in the normal state (curve 2). This nonlinear behavior is probably due to simple heating because we observe an appreciable increase of noise in the differential characteristic dV/dI_t around point C. The dissipated power per unit area at point C is almost as ten times as large as that at point A. Beyond point C, both the nonequilibrium and simple heating effects seem to coexist. For sufficiently large currents, the system exhibits only simple heating effect. The idea of a nonequilibrium state between point B and point C is also supported by the appearance of the fine structures in Figs. 12 and 13. We conclude that the system is still in the nonequilibrium state even after the complete recovery of its normal film resistance.

E. Fine structure

We have often observed nearly periodic fine peaks or wavy structure in the dV/dI_t-vs-I_t characteristic especially when the samples were cooled down below T_λ. Such examples are shown in Fig. 12 for the sample with a glass substrate and Fig. 13 for the sample with a sapphire substrate. It was found that the period of these subpeaks mostly lies in 4–5 mV in tunnel voltage. According to Eq. (19), a peak means a step-function-like increase of the film resistance. The results are possibly related to the phonon effects characteristic to the system in question. A detailed study is under way. The existence of a dynamic resistance is not expected from the theories based on the thermal equilibrium state.

F. Quasiparticle diffusion

It is probable that the quasiparticles injected into the restricted part of a superconducting film diffuse along the film. In order to investigate this effect, we performed the experiment using the junction with a few probes attached to a superconducting film as shown in Fig. 14 similar to the experiment by Hsieh and Levine.[19] The nearest one is located 50 μm apart from the junction edge. We fed a tunnel current I_t and measured the generated

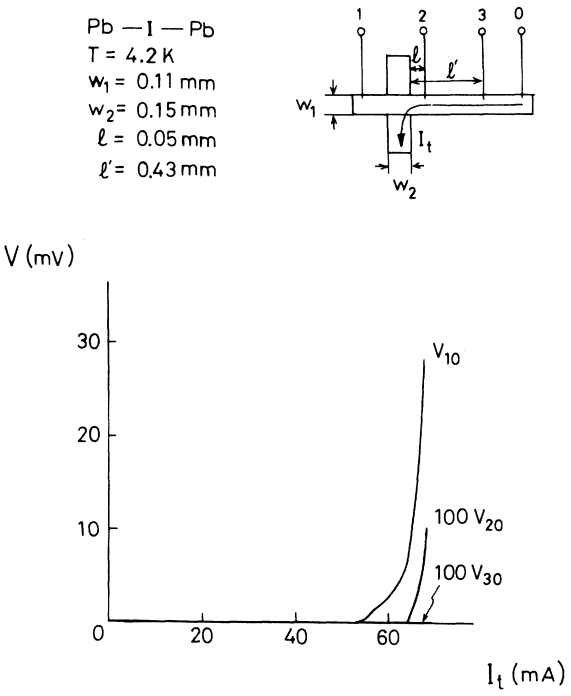

FIG. 14. Experiment to study the quasiparticle diffusion effect. The voltages are measured between the specified two probes.

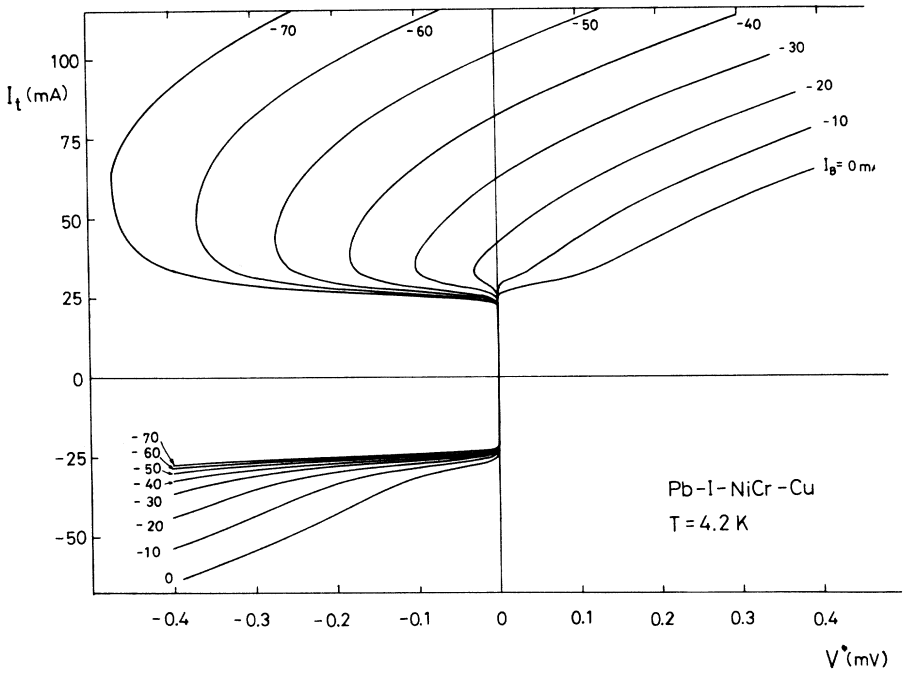

FIG. 15. I_t-V characteristics for various values of bias current I_B for a Pb-I-NiCr-Cu junction.

voltages on the film. While the voltage V_{10} develops rapidly, no voltage is detected between the probe 2 and 3 until V_{10} reached ~5 mV, a magnitude several times as large as that expected from the normal-state film resistance. The result indicates that quasiparticle diffusion is actually small and most of the injected quasiparticles are confined to the junction region. The quasiparticle diffusion length is given by $(v_{qp} l_{qp} \tau_{eff}/3)^{1/2}$, where v_{qp} is an average quasiparticle velocity, l_{qp} is the quasiparticle elastic-scattering mean free path, and τ_{eff} is a characteristic quasiparticle relaxation time.[24] It generally ranges from 0.1 to 10 μm. When the injection rate is high, the quasiparticle diffusion length becomes small. The result is consistent with the above estimate. We do not attribute the appearance of a voltage V_{20} simply to the result of quasiparticle diffusion since a simple heating effect is possibly involved in this current region.

G. Study of the I_t-V characteristic under the influence of a transport current I in the film

In the previous papers,[25,26] we reported many strange characteristics when two independent currents are fed as shown in Fig. 3. These behaviors can be readily interpreted by the four-terminal calculations given in Sec. II B. As an example, consider the I_t-V characteristic with I biased at a

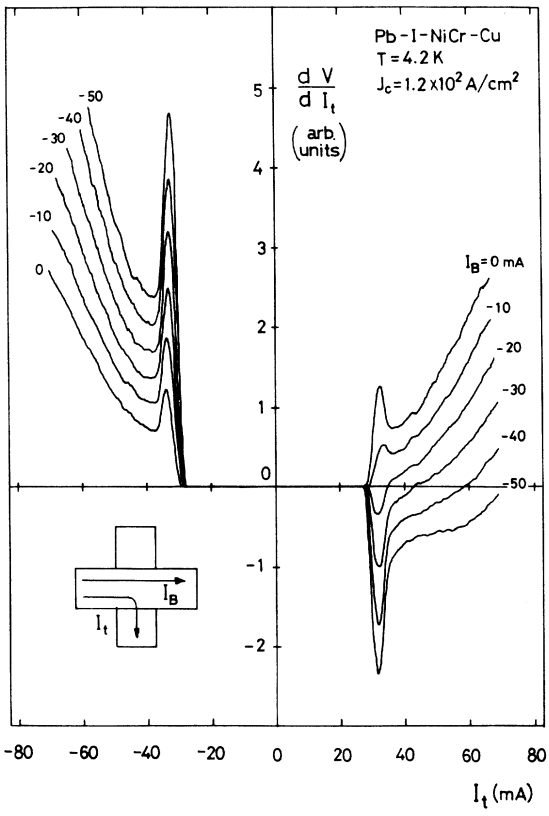

FIG. 16. dV/dI_t characteristics for various values of bias current I_B for Pb-I-NiCr-Cu junction.

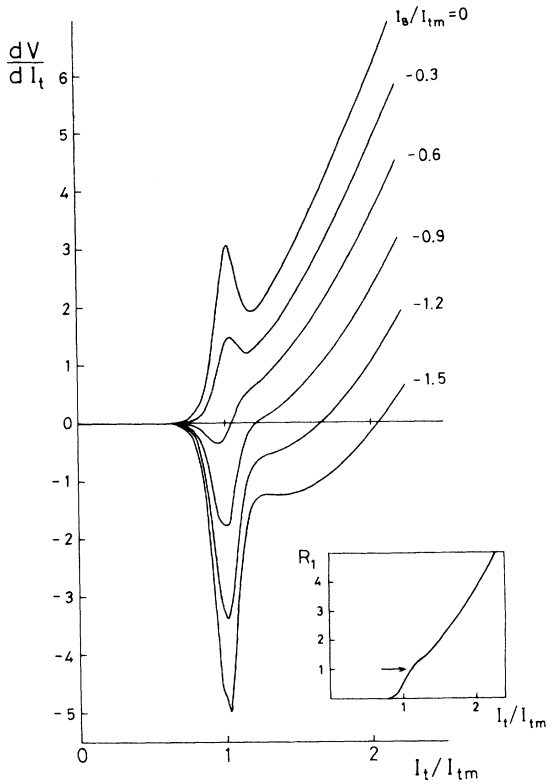

FIG. 17. Calculated dV/dI_t-I_t characteristics for various values of bias current I_B in units of I_{tm}, where I_{tm} is the current value at which R_1 reaches half the value of the normal-state film resistance of the junction part.

constant current I_B. Such a result is again shown in Fig. 15. According to Eq. (20), the voltage V becomes negative provided that I_t and I_B are antiparallel and satisfy the relation $|I_t|<2|I_B|$ for the junctions with $\alpha l \ll 1$, whose behavior is almost observed in Fig. 15. It is more instructive to discuss these data in terms of differential characteristics with respect to I_t. Such experimental curves obtained for various bias currents are given in Fig. 16. The intersecting point with the horizontal axis corresponds to the turning point in Fig. 15. It is important to note that the transition behavior of a superconducting film is hardly affected by the presence of the bias current I_B along the film for the current region $I_B \ll I_c$, supporting the assumption made in Sec. II B. As a four-terminal model calculation, we assume the dependence of R_1 on I_t in the form shown in Fig. 17 which was composed of a smeared step function in the transition region and $I_t^{1.5}$ behavior for higher I_t. The parameters were adjusted so that they fit the observed behavior for R_1 well. The calculated result based on Eq. (22) when I_t and I_B are antiparallel is shown also in Fig. 17. We could successfully reproduce the experimental result by a simple four-terminal calculation here. We have shown that the roles of two currents are clearly separable and only I_t is responsible for the change in superconducting properties for $I_B \ll I_c$.

V. SUMMARY AND CONCLUSIONS

We have studied the nonequilibrium state of superconductors by injecting quasiparticles into a superconducting film through a tunnel barrier and actually demonstrated the destruction of superconductivity by large injection current.

If quasiparticles are injected from a current source into a superconducting film, its effective gap first decreases although it is still in wholly superconducting state. In this process, it is observed that the critical current of the superconducting film decreases with increasing the tunnel current I_t. When I_t reaches a certain critical value I_{tc}, the film enters locally into the nonequilibrium intermediate resistance state. With increasing I_t above I_{tc}, the intermediate resistance rises up to its full value corresponding to the normal-state film resistance. The observed transition width is broad for the samples with sapphire substrates and rather narrow for those with glass substrates, indicating that the resultant nonequilibrium state strongly depends on the phonon escape probability from the sample surface. The broad transition suggests the existence of a spatially inhomogeneous state, which cannot be understood by the theories describing the homogeneous state such as the μ^* or the T^* model. For $T<T_\lambda$, however, we often found a jump at $I_t=I_{tc}$ in the I_t-V characteristic corresponding to a sharp transition of the superconducting film. For further increase of I_t, the film resistance increases, for example, almost linearly with I_t for the samples with sapphire substrates. The additional nearly periodic structures probably associated with phonon effects were sometimes observed in the $dV/dI_t - I_t$ characteristics, showing the possibility of the involvement of a nonthermal effect in this system. The film may be considered as being in the nonequilibrium state in this region and this state lasts until an appreciable simple heating effect is observed.

The theory based on the modified Rothwarf-Taylor equations and Parker's T^* model yields almost the same order of magnitude for the critical tunnel current density J_c for both Pb and Sn junctions. But the dependence of J_c on various parameters is still questionable. The theory also cannot account for the observed gap decrease over the broad range of injection current. In addition, there often appears a first order transition for bath temperatures below T_λ, suggesting that the

system is rather closer to the state predicted by the Owen-Scalapino model in a certain condition.

We conclude that, although the T^* model explains the experimental results under laser irradiation well,[32] it possibly does not apply to the nonequilibrium state formed by quasiparticle injection from an external current source since the injection mechanism is different in both systems and it is necessary to have a new theory which can consistently describe all the phenomena observed in various experimental conditions.

The experiments using two independent currents showed that the roles of the tunnel current I_t and the film transport current I were clearly separable and only the tunnel current was responsible for the change in superconducting properties at least for $I \ll I_c$. This fact leads to the statement that our measurements and those by Wong, Yeh, and Langenberg[24] are almost equivalent because the gap decrease by the transport current itself is small even for $I \sim I_c$.

Several applications are promising utilizing this phenomenon. The application to weak links has been already been demonstrated.[24] It is also useful for the measurement of the effective recombination time.[23] As another application, it may be possible to use this phenomenon as a phonon-generation device. When the tunnel current is biased above I_{tc}, the system is in the nonequilibrium resistive state. If the current is suddenly reduced to zero, a phonon flux of the order of $N(0)\Delta \times d/\tau_{eff}$ is created. It can also be applied to a three-terminal device by feeding two currents as indicated in Figs. 3 and 15. It is noted that the controllability ratio I_{tc}/I_c can be made smaller by reducing the width of the crossing film (see Sec. II A).

ACKNOWLEDGMENTS

The author is indebted to Professor K. Hara, Professor Y. Wada, Professor J. Kondo, and Dr. I. Giaever for valuable comments, Dr. K. H. Gundlach for sending the experimental data, Professor D. N. Langenberg for sending preliminary reports of unpublished work, and Professor. W. H. Parker for private correspondence. He is also thankful to F. Shiota for technical assistance.

[1]There is a review article by D. N. Langenberg, in *Proceedings of the Fourteenth International Conference on Low Temperature Physics*, edited by M. Krusius and M. Vuorio (North-Holland, Amsterdam, 1975), Vol. V, p. 223.
[2]L. R. Testardi, Phys. Rev. B 4, 2189 (1971).
[3]W. H. Parker and W. D. Williams, Phys. Rev. Lett. 28, 1559 (1972).
[4]G. A. Sai-Halsz, C. C. Chi, A. Denenstein, and D. N. Langenberg, Phys. Rev. Lett. 33, 215 (1974).
[5]P. Hu, R. C. Dynes, and V. Narayanamurti, Phys. Rev. B 10, 2786 (1974).
[6]W. H. Parker, Solid State Commun. 15, 1003 (1974).
[7]A. I. Golovashkin, K. V. Mitsen, and G. P. Motulevich, Zh. Eksp. Teor. Fiz. 68, 1408 (1975) [Sov. Phys.-JETP 41, 701 (1976)].
[8]R. Janik, L. Morelli, N. C. Cirillo, Jr., J. N. Lechevet, and W. D. Gregory, IEEE Trans. Mag. MAG-11, 687 (1975).
[9]I. Schuller and K. E. Gray, Phys. Rev. B 12, 2629 (1975).
[10]I. Schuller and K. E. Gray, Phys. Rev. Lett. 36, 429 (1976).
[11]W. Eisenmenger and A. H. Dayem, Phys. Rev. Lett. 18, 125 (1967).
[12]W. Eisenmenger, in *Tunneling Phenomena in Solids*, edited by E. Burstein and S. Lundqvist (Plenum, New York, 1969), p. 371, and the references therein.
[13]H. Kinder, in Ref. 1, Vol. V, p. 287, and the references therein.
[14]D. M. Ginsberg, Phys. Rev. Lett. 8, 204 (1962).
[15]C. J. Adkins, Rev. Mod. Phys. 36, 211 (1964).
[16]B. N. Taylor, Ph.D. thesis (University of Pennsylvania, 1963) (unpublished).
[17]B. I. Miller and A. H. Dayem, Phys. Rev. Lett. 18, 1000 (1967).
[18]J. L. Levine and S. Y. Hsieh, Phys. Rev. Lett. 20, 994 (1968).
[19]S. Y. Hsieh and J. L. Levine, Phys. Rev. Lett. 20, 1502 (1968).
[20]K. E. Gray, A. R. Long, and C. J. Adkins, Philos. Mag. 20, 273 (1969).
[21]K. E. Gray, J. Phys. F 1, 290 (1971).
[22]L. N. Smith and J. M. Mochel, Phys. Rev. Lett. 35, 1597 (1975).
[23]J. T. C. Yeh and D. N. Langenberg (unpublished).
[24]T. Wong, J. T. C. Yeh, and D. N. Langenberg, Phys. Rev. Lett. 37, 150 (1976).
[25]I. Iguchi, The Sixth Conference on Solid State Devices, Digest of Technical Papers, 1974, p. 65 (unpublished); Jpn. J. Appl. Phys. Suppl. 44, 141 (1975).
[26]I. Iguchi, Phys. Lett. A 50, 247 (1974).
[27]I. Iguchi and K. Hara, Phys. Lett. A 59, 313 (1976).
[28]K. H. Gundlach (private communication).
[29]A. F. Hebard, IEEE Trans. Mag. MAG-11, 358 (1975).
[30]C. S. Owen and D. J. Scalapino, Phys. Rev. Lett. 28, 1559 (1972).
[31]J-J. Chang and D. J. Scalapino, Phys. Rev. B 9, 4769 (1974).
[32]W. H. Parker, Phys. Rev. B 12, 3667 (1975).
[33]V. G. Baru and A. A. Sukhanov, Zh. Eksp. Teor. Fiz. Pis. Red. 21, 209 (1975) [JETP Lett. 21, 93 (1975)].
[34]A. Rothwarf and B. N. Taylor, Phys. Rev. Lett. 19, 27 (1967).
[35]A. Rothwarf, G. A. Sai-Halasz, and D. N. Langenberg, Phys. Rev. Lett. 33, 212 (1974).
[36]With this approximation, we are probably estimating

the upper limt for the phonon production with energy greater than 2Δ.

[37]S. B. Kaplan, C. C. Chi, D. N. Langenberg, J-J Chang, S. Jafarey, and D. J. Scalapino, Phys. Rev. B 14, 4854 (1976).

[38]A. R. Long and C. J. Adkins, Philos. Mag. 27, 865 (1973).

[39]W. Eisenmenger and K. Lassmann (unpublished).

[40]J. I. Gittleman and S. Bozowski, Phys. Rev. 128, 646 (1962).

[41]In Ref. 27, we did not take into account the high energy effect of injected quasiparticles, which resulted in rather low η to fit the experimental data. The numerical values for $J_c(T)/J_c(0)$ in Ref. 27, however, closely lies in those obtained from Eq. (7).

[42]W. H. Parker (private communication).

[43]J. Bardeen, Rev. Mod. Phys. 34, 667 (1962).

[44]V. L. Newhouse, *Applied Superconductivity* (Wiley, New York, 1964).

[45]R. J. Pedersen and F. L. Vernon, Jr., Appl. Phys. Lett. 10, 29 (1967).

[46]I. Giaever, *Tunneling Phenomena in Solids*, edited by E. Burnstein and S. Lundqvist (Plenum, New York, 1969), p. 19.

[47]J. M. Rowell, A. G. Chynoweth, and J. C. Phillips, Phys. Rev. Lett. 9, 59 (1962).

[48]B. N. Brockhouse, T. Arase, G. Caglioti, K. R. Rao, and A. D. B. Woods, Phys. Rev. 128, 1099 (1962).

[49]J. M. Rowell, P. W. Anderson, and D. E. Thomas, Phys. Rev. Lett. 10, 334 (1963).

[50]J. M. Rowell and L. Kopf, Phys. Rev. 137, 907 (1965).

[51]G. Burrafato, G. Faraci, G. Giaquinta, and N. A. Mancini, J. Phys. C 5, 2179 (1972).

[52]During the course of work we ruled out the other possible mechanisms such as flux flow or proximity effect, etc., experimentally.